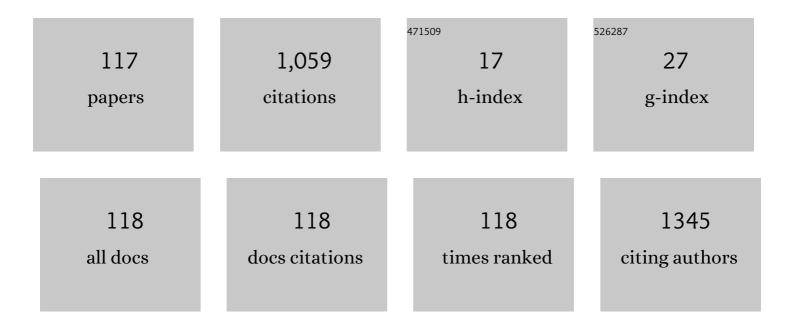
## George A Stanciu

List of Publications by Year in descending order

Source: https://exaly.com/author-pdf/6031024/publications.pdf Version: 2024-02-01



#	Article	IF	CITATIONS
1	Experimenting Liver Fibrosis Diagnostic by Two Photon Excitation Microscopy and Bag-of-Features Image Classification. Scientific Reports, 2014, 4, 4636.	3.3	55
2	Inhibitory Activity of \${m Fe}_{3} {m O}_{4}\$/Oleic Acid/Usnic Acid—Core/Shell/Extra-Shell Nanofluid on S. aureus Biofilm Development. IEEE Transactions on Nanobioscience, 2011, 10, 269-274.	3.3	53
3	Corrosion resistance appraisal of TiN, TiCN and TiAlN coatings deposited by CAE-PVD method on WC–Co cutting tools exposed to artificial sea water. Applied Surface Science, 2015, 358, 572-578.	6.1	52
4	Efficiency of Vanilla, Patchouli and Ylang Ylang Essential Oils Stabilized by Iron Oxide@C14 Nanostructures against Bacterial Adherence and Biofilms Formed by Staphylococcus aureus and Klebsiella pneumoniae Clinical Strains. Molecules, 2014, 19, 17943-17956.	3.8	49
5	Characterization of Langmuir–Blodgett films of a calix[8]arene and sensing properties towards volatile organic vapors. Sensors and Actuators B: Chemical, 2010, 148, 358-365.	7.8	48
6	Improved quantification of collagen anisotropy with polarizationâ€resolved second harmonic generation microscopy. Journal of Biophotonics, 2017, 10, 1171-1179.	2.3	38
7	Hybrid Nanomaterial for Stabilizing the Antibiofilm Activity of Eugenia carryophyllata Essential Oil. IEEE Transactions on Nanobioscience, 2012, 11, 360-365.	3.3	36
8	Antimicrobial Activity Evaluation on Silver Doped Hydroxyapatite/Polydimethylsiloxane Composite Layer. BioMed Research International, 2015, 2015, 1-13.	1.9	36
9	Quantitative second harmonic generation microscopy for the structural characterization of capsular collagen in thyroid neoplasms. Biomedical Optics Express, 2018, 9, 3923.	2.9	31
10	The influence of the surface morphologies of Langmuir Blodgett (LB) thin films of porphyrins on their gas sensing properties. Sensors and Actuators B: Chemical, 2011, 158, 62-68.	7.8	30
11	High-resolution quantitative determination of dielectric function by using scattering scanning near-field optical microscopy. Scientific Reports, 2015, 5, 11876.	3.3	28
12	Nanoscale mapping of refractive index by using scattering-type scanning near-field optical microscopy. Nanomedicine: Nanotechnology, Biology, and Medicine, 2018, 14, 47-50.	3.3	26
13	Structural characterization and adhesion appraisal of TiN and TiCN coatings deposited by CAE-PVD technique on a new carbide composite cutting tool. Journal of Adhesion Science and Technology, 2015, 29, 2576-2589.	2.6	25
14	Pulsed laser deposition of lead-free (Na0.5Bi0.5)1â^'xBaxTiO3 ferroelectric thin films with enhanced dielectric properties. Applied Surface Science, 2013, 278, 162-165.	6.1	24
15	Nanostructured bioglass thin films synthesized by pulsed laser deposition: CSLM, FTIR investigations and in vitro biotests. Applied Surface Science, 2008, 255, 3056-3062.	6.1	23
16	Correlative imaging of biological tissues with apertureless scanning near-field optical microscopy and confocal laser scanning microscopy. Biomedical Optics Express, 2017, 8, 5374.	2.9	19
17	Automated compensation of light attenuation in confocal microscopy by exact histogram specification. Microscopy Research and Technique, 2010, 73, 165-175.	2.2	17
18	A study on the image contrast of pseudo-heterodyned scattering scanning near-field optical microscopy. Optics Express, 2014, 22, 1687.	3.4	17

#	Article	IF	CITATIONS
19	Nonlinear optical imaging of defects in cubic silicon carbide epilayers. Scientific Reports, 2014, 4, 5258.	3.3	17
20	Optical properties of Sm3+ doped strontium hexa-aluminate single crystals. Journal of Alloys and Compounds, 2015, 622, 296-302.	5.5	17
21	Enamel Based Composite Layers Deposited on Titanium Substrate with Antifungal Activity. Journal of Spectroscopy, 2016, 2016, 1-13.	1.3	17
22	Highly transparent Yb:Y2O3 ceramics obtained by solid-state reaction and combined sintering procedures. Ceramics International, 2019, 45, 3217-3222.	4.8	17
23	Structural and optical properties of Mn doped ZnS semiconductor nanostructures. Indian Journal of Physics, 2010, 84, 1361-1367.	1.8	15
24	On the Suitability of SIFT Technique to Deal with Image Modifications Specific to Confocal Scanning Laser Microscopy. Microscopy and Microanalysis, 2010, 16, 515-530.	0.4	14
25	Influence of Confocal Scanning Laser Microscopy specific acquisition parameters on the detection and matching of Speeded-Up Robust Features. Ultramicroscopy, 2011, 111, 364-374.	1.9	14
26	Characterization of Nanomaterials by Locally Determining Their Complex Permittivity with Scattering-Type Scanning Near-Field Optical Microscopy. ACS Applied Nano Materials, 2020, 3, 1250-1262.	5.0	14
27	Incongruent Melting La <sub><i>x</i></sub> Y <sub><i>y</i></sub> Sc <sub>4-x-y</sub> (BO <sub>3</sub> ) <sub>4</sub> : LYSB Nonlinear Optical Crystal Grown by the Czochralski Method. ACS Applied Materials & Interfaces, 2019. 11. 20987-20994.	8.0	13
28	Electrochemical stability and surface analysis in evaluation fluoride effect on new bioalloy Ti7Al3V2Mo2Fe used in dentistry. Materials and Corrosion - Werkstoffe Und Korrosion, 2011, 62, 1111-1116.	1.5	11
29	The interaction between the gas sensing and surface morphology properties of LB thin films of porphyrins in terms of the adsorption kinetics. Materials Chemistry and Physics, 2012, 136, 1130-1136.	4.0	11
30	Combined far-field, near-field and topographic imaging of nano-engineered polyelectrolyte capsules. Materials Letters, 2016, 183, 105-108.	2.6	11
31	SSNOMBACTER: A collection of scattering-type scanning near-field optical microscopy and atomic force microscopy images of bacterial cells. GigaScience, 2020, 9, .	6.4	11
32	Scanning probe microscopy, luminescence and third harmonic generation studies of elongated CdS:Mn nanostructures developed by energetic oxygen-ion-impact. EPJ Applied Physics, 2006, 35, 29-36.	0.7	10
33	Influence of atomic force microscopy acquisition parameters on thin film roughness analysis. Microscopy Research and Technique, 2012, 75, 921-927.	2.2	10
34	Identification of stacking faults in silicon carbide by polarization-resolved second harmonic generation microscopy. Scientific Reports, 2017, 7, 4870.	3.3	10
35	Objective analysis of collagen organization in thyroid nodule capsules using second harmonic generation microscopy images and the Hough transform. Applied Optics, 2020, 59, 6925.	1.8	10
36	Detector array incorporated optical scattering instrument for nephelometric measurements on small particles. Measurement Science and Technology, 2009, 20, 095901.	2.6	9

#	Article	IF	CITATIONS
37	Surface Charge and Carbon Contamination on an Electron-Beam-Irradiated Hydroxyapatite Thin Film Investigated by Photoluminescence and Phase Imaging in Atomic Force Microscopy. Microscopy and Microanalysis, 2014, 20, 586-595.	0.4	9
38	Bifunctional LaxNdyGdzSc4â^'xâ^'yâ^'z(BO3)4 crystal: Czochralski growth, linear and nonlinear optical properties, and near-infrared laser emission performances. Optics and Laser Technology, 2020, 131, 106433.	4.6	9
39	Influence of hematoxylin and eosin staining on the quantitative analysis of second harmonic generation imaging of fixed tissue sections. Biomedical Optics Express, 2021, 12, 5829.	2.9	9
40	Magnetic Nanoparticles for Controlling in vitro Fungal Biofilms. Current Organic Chemistry, 2013, 17, 1023-1028.	1.6	9
41	Scattering-type Scanning Near-Field Optical Microscopy of Polymer-Coated Gold Nanoparticles. ACS Omega, 2022, 7, 11353-11362.	3.5	9
42	Electron beam influence on the carbon contamination of electron irradiated hydroxyapatite thin films. Applied Surface Science, 2015, 346, 342-347.	6.1	8
43	Pyramidal growth of ceria nanostructures by pulsed laser deposition. Applied Surface Science, 2016, 363, 245-251.	6.1	8
44	Spectroscopic investigations of Pr3+ ions doped CNGG and CLNGG single crystals. Journal of Alloys and Compounds, 2019, 799, 288-301.	5.5	8
45	Characterization of a Novel 1,3-Bis( <i>p</i> -iminobenzoic acid)indane Langmuir-Blodgett Film for Organic Vapor Sensing. Journal of Nanoscience and Nanotechnology, 2005, 5, 1108-1112.	0.9	7
46	Mapping electron-beam-injected trapped charge with scattering scanning near-field optical microscopy. Optics Letters, 2016, 41, 1046.	3.3	7
47	Growth Mechanisms and the Effects of Deposition Parameters on the Structure and Properties of High Entropy Film by Magnetron Sputtering. Materials, 2019, 12, 3008.	2.9	7
48	Pixelâ€level angular quantification of capsular collagen in second harmonic generation microscopy images of encapsulated thyroid nodules. Journal of Biophotonics, 2020, 13, e202000262.	2.3	7
49	Formation of Langmuir–Blodgett thin film of a novel N-dodecylphthalimide. Materials Letters, 2006, 60, 2371-2374.	2.6	6
50	Investigation on Photonic-Corral-Mode Quantum Ring Lasers by Laser Scanning Microscopy. , 2008, , .		6
51	Two Photon Emission and Nonlinear Optical Imaging of Acetonitrile-Treated Quasi-Spherical Nanoscale PbS Systems. IEEE Photonics Journal, 2010, 2, 1060-1068.	2.0	6
52	Improving the Properties of CdS Nanoparticles by Adding Polymers. Particulate Science and Technology, 2011, 29, 229-241.	2.1	5
53	Blue light production by type-I non-critical phase matching second-harmonic generation in La(Ca <sub>1â^'x</sub> Sr <sub>x</sub> ) <sub>4</sub> O(BO <sub>3</sub> ) <sub>3</sub> single crystals. CrystEngComm, 2015, 17, 4098-4101.	2.6	5
54	Perspectives on combining Nonlinear Laser Scanning Microscopy and Bag-of-Features data classification strategies for automated disease diagnostics. Optical and Quantum Electronics, 2016, 48, 1.	3.3	5

#	Article	IF	CITATIONS
55	PSHG-TISS: A collection of polarization-resolved second harmonic generation microscopy images of fixed tissues. Scientific Data, 2022, 9, .	5.3	5
56	Vapour growth and characterization of HgBr2crystals using confocal laser scanning microscopy, optical spectroscopy and DC conductivity measurements. Journal Physics D: Applied Physics, 1999, 32, 1928-1933.	2.8	4
57	Optical beam induced current microscopy of photonic quantum ring lasers. Applied Physics B: Lasers and Optics, 2011, 103, 653-657.	2.2	4
58	Digital image inpainting and microscopy imaging. Microscopy Research and Technique, 2011, 74, 1049-1057.	2.2	4
59	Investigations on SiC by using nonlinear effects in scanning laser microscopy. , 2011, , .		4
60	Multispectral detection of cutaneous lesions using spectroscopy and microscopy approaches. , 2018, , .		4
61	Near field investigation based on a novel apertureless near field optical microscope. , 2009, , .		3
62	Construction of a multidetector array incorporated laser-based scattering system for ultrafine TiO2 characterization. Journal of Optics (India), 2009, 38, 67-74.	1.7	3
63	Automatic estimation of stacking fault density in SiC specimens imaged by transmission electron microscopy. , 2011, , .		3
64	Nonlinear optical effects used for investigations on biological samples at micro and nanoscale. , 2016, , .		3
65	Changes in the Collagen Structure of Thyroid Nodule Capsules Determined by Polarization-Resolved Second Harmonic Generation Microscopy. , 2018, , .		3
66	Comparison of Vacancy Sink Efficiency of Cu/V and Cu/Nb Interfaces by the Shared Cu Layer. Materials, 2019, 12, 2628.	2.9	3
67	Langmuir–Blodgett film properties of based on calix[4]resorcinarene and the detection of those against volatile organic compounds. Applied Physics A: Materials Science and Processing, 2019, 125, 1.	2.3	3
68	Strategies for Optimizing the Determination of Second-Order Nonlinear Susceptibility Tensor Coefficients for Collagen in Histological Samples. IEEE Access, 2019, 7, 135210-135219.	4.2	3
69	Surface optical characterization at nanoscale using phasor representation of data acquired by scattering scanning near-field optical microscopy. Applied Surface Science, 2020, 509, 145347.	6.1	3
70	Multi-Level Evaluation of UV Action upon Vitamin D Enhanced, Silver Doped Hydroxyapatite Thin Films Deposited on Titanium Substrate. Coatings, 2021, 11, 120.	2.6	3
71	Gas Sensing Properties of Porphyrin Thin Films Influenced by Their Surface Morphologies. Sensor Letters, 2014, 12, 1218-1227.	0.4	3
72	Growth and characterization of 3.5 at.% Nd:LGSB bifunctional crystal. Optical Materials, 2022, 123, 111832.	3.6	3

#	Article	IF	CITATIONS
73	Investigation of HgBr x I 2-x using confocal laser scanning microscopy and x-ray diffraction. , 1998, 3405, 241.		2
74	Photonic-Corral-Mode Quantum Ring Lasers investigated by Laser Scanning Microscopy and Near Field Microscopy. , 2008, , .		2
75	Tunneling at emitter periphery in silicon nitride passivated InP/InGaAs HBTs. , 2008, , .		2
76	Hydroxyapatite surface charge investigated by scanning probe microscopy. , 2014, , .		2
77	Bags of features for classification of Laser Scanning Microscopy data. , 2015, , .		2
78	A New Technique in Scanning Near Field Optical Microscopy Used for Investigations on the Biological Samples. , 2018, , .		2
79	(INVITED) Czochralski-grown LaxGdyRzSc4-x-y-z(BO3)4 (R = Yb, Nd) crystals - A review of recent developments. Optical Materials: X, 2020, 7, 100052.	0.8	2
80	Assessment of Extramammary Paget Disease by Two-Photon Microscopy. Frontiers in Medicine, 2022, 9, 839786.	2.6	2
81	<title>Nanometrology of microsystems: traceability problem in nanometrology</title> . , 2007, , .		1
82	Image fusion for photonic quantum ring laser structures investigated by confocal scanning laser microscopy. , 2009, , .		1
83	Metallic samples investigated by using a scattering near field optical microscope. , 2012, , .		1
84	Growth of CdS nanoparticles in Y- and Z-type Langmuir–Blodgett thin film using 1,3-bis-(p-iminobenzoic) Tj ET	Qq0 0 0 r	gBT <sub>1</sub> /Overlock
85	Investigations at nanoscale by using fluorescence in apertureless scanning near field microscopy. , 2013, , .		1
86	Investigations on organic fluorophore doped silica nanoparticles by apertureless scanning near-field optical microscopy. , 2014, , .		1
87	Fractal analysis correlation of the images from scanning laser microscopy techniques and atomic force microscopy. , 2017, , .		1
88	Correlative investigations of biological specimens using label free far-field and near-field microscopy techniques. , 2017, , .		1
89	Nanoscale Investigations of Optical Fiber by Using Scattering Scanning Near-Field Optical Microscopy. , 2018, , .		1

90Calix [4] amine Langmuir-Blodgett thin film sensing properties against volatile organic compounds.0.4190Journal of Physics: Conference Series, 2019, 1186, 012011.0.41

#	Article	IF	CITATIONS
91	Correlative Imaging Using a Multimodal Microscopy System for Investigations at Micro and Nano Scales. , 2019, , .		1
92	Matching DSIFT Descriptors Extracted from CSLM Images. Engineering, 2013, 05, 199-202.	0.8	1
93	Pr:LCSB as a new nonlinear optical crystal: Czochralski growth and optical characterization. Journal of Alloys and Compounds, 2022, 908, 164633.	5.5	1
94	<title>3D images used in the localization of the defects in semiconductor devices</title> . , 1994, 2184, 127.		0
95	<title>Display and analysis of 2D and 3D images obtained on semiconductor devices using a laser scanner</title> . , 1994, 2337, 78.		Ο
96	Nonlinear conduction in platinum nanoparticle films. , 0, , .		0
97	Investigations on the variable large bandgap semiconductor compound HgBrl. Journal Physics D: Applied Physics, 2003, 36, 2714-2718.	2.8	Ο
98	Surface investigations on HgBr <sub>2</sub> single crystals by using confocal scanning laser microscopy. Scanning, 2000, 22, 182-186.	1.5	0
99	Atomic force microscopy analysis of orientation effect on InP-based heterojunction bipolar transistors. , 2007, , .		0
100	Investigation on CdS: Mn quantum dots using scanning laser microscopy. , 2007, , .		0
101	<title>Study of hydroxyl carbonate apatite formation on bioactive glass coated dental ceramics by confocal laser scanning microscopy (CLSM)</title> . , 2007, , .		0
102	Chromium Doped ZnS Nanostructures: Structural and Optical Characteristics. , 2009, , .		0
103	Scanning laser microscopy: From far field to near field. , 2009, , .		Ο
104	Feature based recognition of photonic devices in images obtained by confocal scanning laser microscopy. , 2009, , .		0
105	Optical induced current technique used to investigate the photonic quantum ring laser. , 2010, , .		0
106	Two-photon excited photoluminescence of photonic quantum ring laser structures. Applied Physics B: Lasers and Optics, 2012, 107, 97-101.	2.2	0
107	On packing laser scanning microscopy images by reversible watermarking: A case study. , 2015, , .		0
108	Bag-of-features approaches for combined classification of laser scanning microscopy and spectroscopy data sets. , 2016, , .		0

#	Article	IF	CITATIONS
109	Transparent Nd doped YAG ceramics. Journal of Physics: Conference Series, 2016, 741, 012074.	0.4	Ο
110	Nonlinear optical microscopy for investigation of gastrointestinal lesions. Proceedings of SPIE, 2017, ,	0.8	0
111	Nanoscale imaging by using label free microscopy techniques. , 2017, , .		Ο
112	Advances in Fractal Analysis of the Biological Tissues Images Obtained by Using Laser Scanning Microscopy. , 2019, , .		0
113	Advanced NLO Crystals for Efficient Blue Laser Sources Based on SHG Processes. , 2015, , .		0
114	Laser Gain Transparent Ceramics Media. , 2017, , .		0
115	Imaging Biological Specimens and Advanced Materials with Correlative Far-field Near-field Microscopy. , 2018, , .		0
116	Quantitative imaging of advanced nanostructured materials with scattering-type scanning near field optical microscopy. , 2019, , .		0
117	LYSB and Yb-doped LYSB Crystals: Czochralski Growth, Optical Characterization and Laser Emission Performances. , 2021, , .		0